

Molecular dynamics simulation for ternary lithium-aluminium-phosphate glass

E. M. ROTIU, B. A. SAVA*, M. ELISA^a

National Institute of Glass, 47th Th. Pallady Av., Sect.3, 032258, Bucharest, Romania

^aDepartment of Optospintronics, National Institute of Optoelectronics-INOE 2000, 1st Atomistilor Street, P.O. Box MG - 5, RO-77125, Com. Magurele, Romania

P₂O₅-Al₂O₃-Li₂O vitreous system structure was simulated by molecular dynamic (MD) method. The knowledge of analytical formula of the interaction forces enables, for a limited number of ions, to solve the Newtonian equations, which describe the particles movement. The simulation gives atomic system configuration images, at several temperatures, starting at 3000K, down to 1000K, 700K and 300K temperatures. Information about glass structure was determined by calculation of radial distribution function. The maxima from the radial distribution function represent the most likely distances between two ionic species.

(Received February 02, 2009; accepted September 30, 2009)

Keywords: Molecular dynamics simulation, Phosphate glass, Lithium oxide, Aluminium oxide

1. Introduction

Computer simulation of atomic or ionic movements in liquid phase allows easily obtaining states of fact similar to glass. The structure of those simulated glass corresponds however to very elevated fictive temperatures and to a very high cooling rate. Molecular dynamic (MD) study of a 500 spheres ensemble leads to the obtaining of radial distribution function identical to the Bernal one (radial distribution function for up to 3000 disordered compact spheres, having 0,637 rumpling coefficient and the number of vicinity contact spheres between 5 and 12, average number 8 – comparable to compact crystalline structures).

Woodcock [1] studied spheres systems according to Lenard-Jones potential, ionic systems and systems which form network similar to that of vitreous silica. The model is in good agreement with the experimental data.

Hirao and Soga developed MD method, using the Born-Mayer-Huggins (BMH) potential as follows [1]:

$$\Phi_{ij(r)} = \frac{Z_i Z_j e^2}{r} + \left(1 + \frac{Z_i}{n_i} + \frac{Z_j}{n_j}\right) b_{ij} \exp[(\sigma_i + \sigma_j - r_{ij})/\rho] \quad (1)$$

where: Z = electronic number;

n = valence electron number;

b and ρ = constants;

σ = distance parameter.

The characteristic values obtained for soda-silicate glass are presented in Table 1.

Table 1. The calculated values by MD method.

Composition	Temperature (K)	Si-O		O-O	
		r _{Si-O} (Å)	N _{Si-O} (atoms)	r _{O-O} (Å)	N _{O-O} (atoms)
2Li ₂ O.SiO ₂	2000	1,55	4,5	2,65	3,3
2Li ₂ O.SiO ₂	605	1,60	4,0	2,65	3,6
2Na ₂ O.SiO ₂	601	1,61	4,1	2,66	4,1
2K ₂ O.SiO ₂	603	1,62	4,1	2,66	4,4

Boiko and others used MD method based on calculation of atomic interaction according to Pauling's ionic force law [2].

$$F(r_{ij}) = \frac{q_i q_j}{r_{ij}} \left[\text{sign}(q_i q_j) - \left(\frac{r_i + r_j}{r_{ij}} \right)^n \right] \quad (2)$$

where: F(r_{ij}) = force between i and j ions, situated at r_{ij} distance;

q_i = particle charge;

r_i = particle radius;

n = repulsive characteristic.

The obtained data for Na₂O-SiO₂ melts, in comparison with experimental ones, are presented in Table 2.

Table 2. Calculated MD values, in comparison with experimental data.

Ions pairs	Experimental, melt at 1400°C		MD model, 1620 K	
	r _{ij} , Å	N _{ij}	r _{ij} , Å	N _{ij}
Si-O	1,61	3,9	1,62	4
O-O	2,65	5,8	2,61	4,2
Si-Si	3,22	3,1	3,18	2,3
Na-O	2,34	5,5	2,28	5

Benino, Soga and Hirao [3] used, for MD calculation, interatomic potentials described by Gilbert-Ida type function, with r^{-6} terms, as follows:

$$\Phi_{ij(r)} = \frac{e^2}{4\pi\epsilon_0} \frac{Z_i Z_j}{r_{ij}} + f_0 (b_i + b_j) \exp\left(\frac{a_i + a_j - r_{ij}}{b_i + b_j}\right) - \frac{e_i e_j}{r_{ij}^6} \quad (3)$$

where: Z = electronic number of ion;
 a , b and c = characteristic parameters for each element;
 f_0 = normalization constant.

Iwamoto and others [4] used, for MD simulation, one repulsive term and one simplified coulombian interaction:

$$\Phi_{ij(r)} = Z_i Z_j \frac{e^2}{r} + f_0 (b_i + b_j) \exp\left(\frac{a_i + a_j - r_{ij}}{b_i + b_j}\right) \quad (4)$$

where: Z_i = electronic number of ion;
 e = unitary charge;
 f_0 = force constant;
 a_i and b_i = radius and compressibility for i ion.

Soules [5] performed MD computations using a simple formula for interionic potentials, comprising a repulsive part and a coulombian attraction potential:

$$V_{ij(r)} = \frac{a_{ij}}{r^n} + \frac{z_i z_j e^2}{r} \quad (5)$$

$$V_{ij(r)} = A_{ij} e^{-\frac{r}{\rho}} + \frac{z_i z_j e^2}{r} \quad (6)$$

2. Modeling

MD method [6-9] simulates glass structure knowing the atomic interaction forces. These forces are derived from a certain type of potential. The knowledge of analytical formula for the interaction forces enables, for a reasonable number of ions, to solve Newtonian equations for the particles system movement. In other words, if the initial positions and speeds of ions are known, it is possible to calculate the positions (and speeds) at ulterior moment. The ions are considered to be distributed in a cube whose dimension depends on their number and density of glass. The elementary cell dimension was deduced as a function of atoms number and system density, 2500 kg/m^3 . Ions speeds are considered Maxwell distributed, corresponding to one given temperature:

$$\frac{3}{2} NkT = \sum_{i=1}^N \frac{m_i v^2}{2} \quad (9)$$

The positions will be calculated from Newtonian equation system:

$$F_i = m_i \frac{d^2 r_i}{dt^2} \quad (10)$$

The simulation is based on Born-Mayer potential:

$$\Phi_{ij} = \frac{1}{4\pi\epsilon_0} \frac{Z_i Z_j}{r_{ij}} + B_{ij} \exp\left(-\frac{r_{ij}}{\rho_{ij}}\right) \quad (11)$$

where: r is the interatomic distance, Z the effective charge, B and ρ are constants presented in Table 3.

Table 3. Interaction constants.

Type of interaction	B[eV]	$\rho[\text{\AA}^{-1}]$
O-O	2644.8	3.4
Li-Li	167.47	3.4
Li-P	158.09	3.4
Li-O	300.00	3.4
P-P	148.93	3.4
Li-Al	510.625	3.4
P-O	694.66	3.4
Al-Al	1039.5842	3.4
O-Al	1725.0881	3.4
Al-P	600.32	3.4

The simulation starts from a random configuration, at initial temperature of 3000K. The composition of simulated glass is 72% P_2O_5 , 19% Al_2O_3 , 9% Li_2O . The system evolved for 40 ps (40000 iterations). The final configuration was considered as initial for 1000K temperature. The process restarted for 700K and 300K temperatures. In the simulation process, 6260 ions from which 4260 oxygen, 1440 phosphorus, 380 aluminum and 180 lithium, have been considered.

3. Results and discussion

Figs. 1-4 present images of the ionic distribution for the above-mentioned four temperatures (green-Al, red-O, brown-P, and gray-Li).

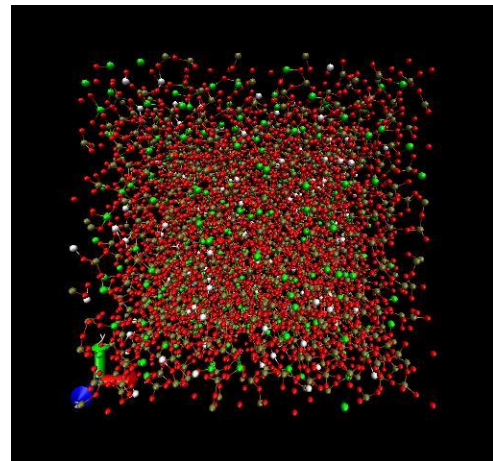


Fig. 1. System image at 3000 K temperature.

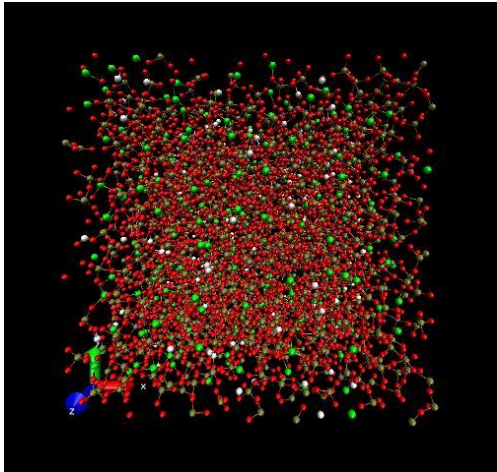


Fig. 2. System image at 1000K temperature.

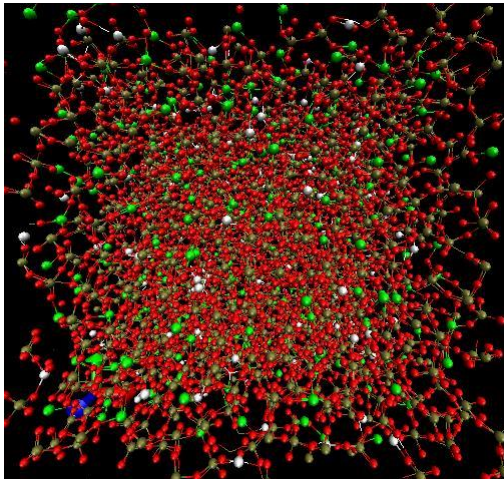


Fig. 3. System image at 700K temperature.

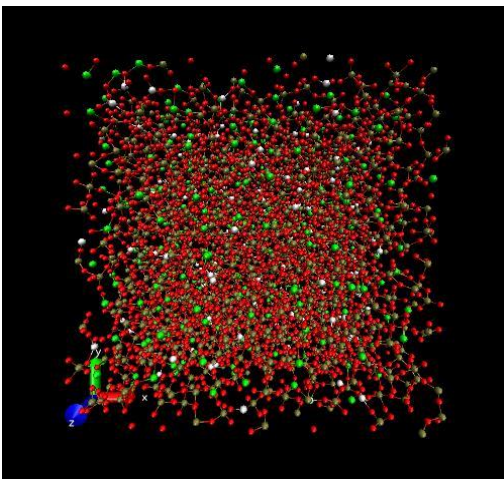


Fig. 4. System image at 300K temperature.

Glass structure was determined by calculation of radial distribution function, for ion pairs. For two i and j ionic species, it defines:

$$g_{ij}(r) = \left\langle \frac{1}{N\rho} \sum_i \sum_{j \neq i} \delta[r - r_{ij}] \right\rangle \quad (12)$$

where N is the particle number, r_{ij} the distance between considered particles, ρ is the system density. The position of maxima from the radial distribution function represents the most likely distances between two ionic species.

Figs. 5-16 presents the radial distribution function corresponding to the four simulation temperatures.

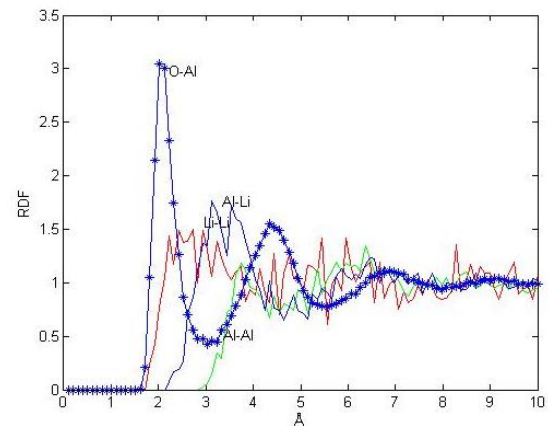


Fig. 5. Radial distribution functions for O-Al, Al-Li, Al-Al and Li-Li interaction, at 3000K.

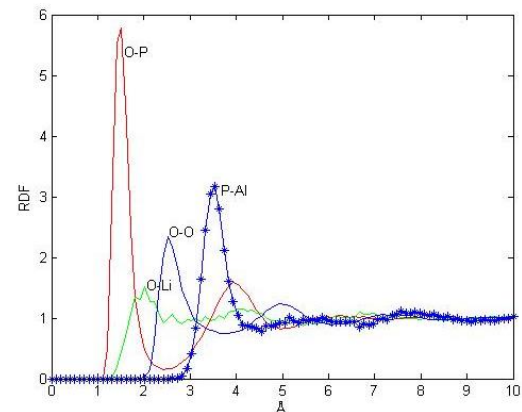


Fig. 6. Radial distribution functions for O-Li, P-Al, O-P and O-O interaction, at 3000K.

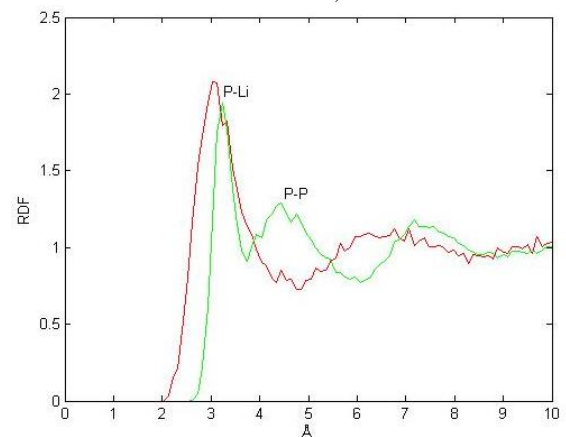


Fig. 7. Radial distribution functions for P-P and P-Li interaction, at 3000K.

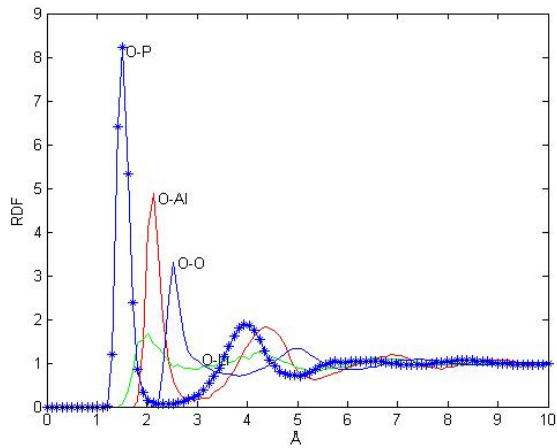


Fig. 8. Radial distribution functions for O-Al, O-P, O-Li and O-O interaction, at 1000K.

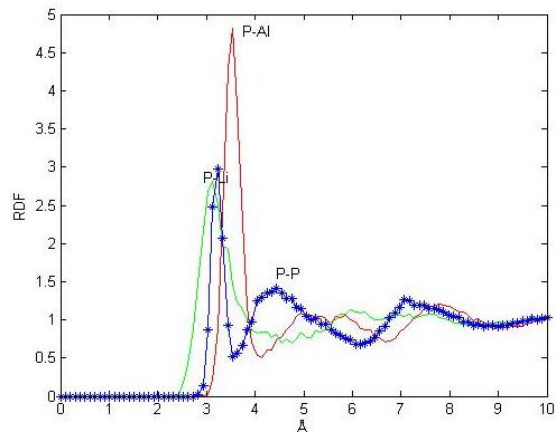


Fig. 9. Radial distribution functions for P-Al, P-P and P-Li interaction, at 1000K.

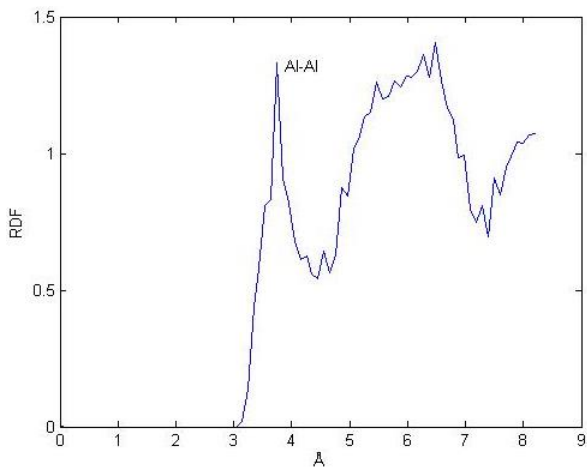


Fig. 10. Radial distribution functions for Al-Al interaction, at 1000K.

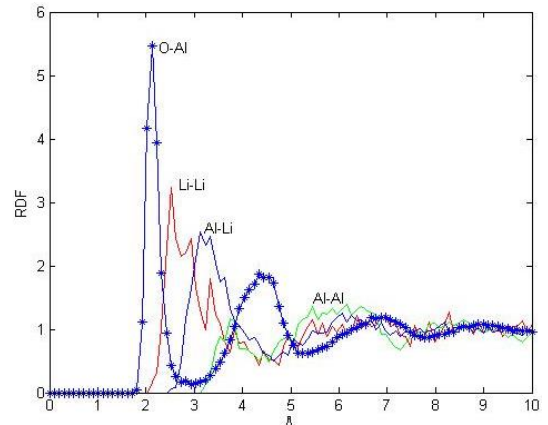


Fig. 11. Radial distribution functions for O-Al, Li-Li, Al-Li, and Al-Al interaction, at 700K.

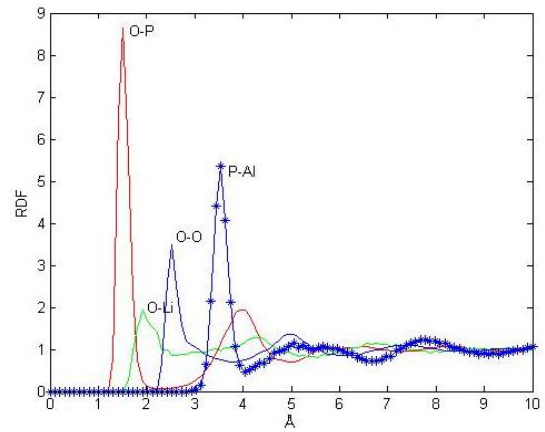


Fig. 12. Radial distribution functions for O-P, O-Li, O-O, and P-Al interaction, at 700K.

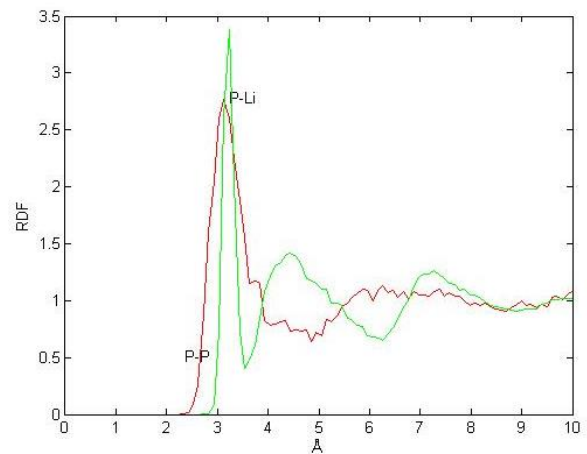


Fig. 13. Radial distribution functions for P-P and P-Li interaction, at 700K.

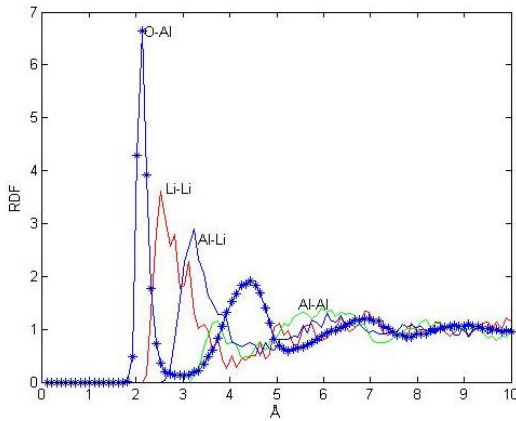


Fig. 14. Radial distribution functions for O-Al, Li-Li, Al-Li, and Al-Al interaction, at 300K.

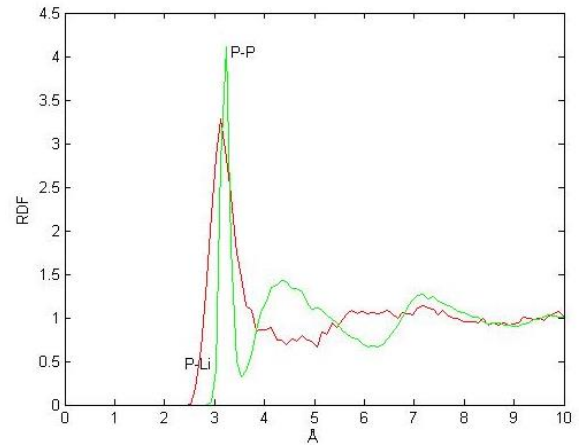


Fig. 16. Radial distribution functions for P-Li and P-P interaction, at 300K.

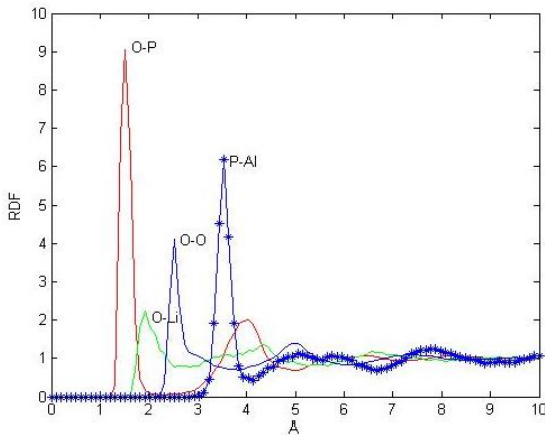


Fig. 15. Radial distribution functions for O-P, O-Li, O-O, and P-Al interaction, at 300K.

Fig. 17 presents the total distribution functions at three temperatures. The lowest curve corresponds to 3000 K and the highest one to 300 K. The increasing of radial distribution curves area indicates that by simulated cooling, the coordination spheres are stabilized, corresponding to the amorphous structure.

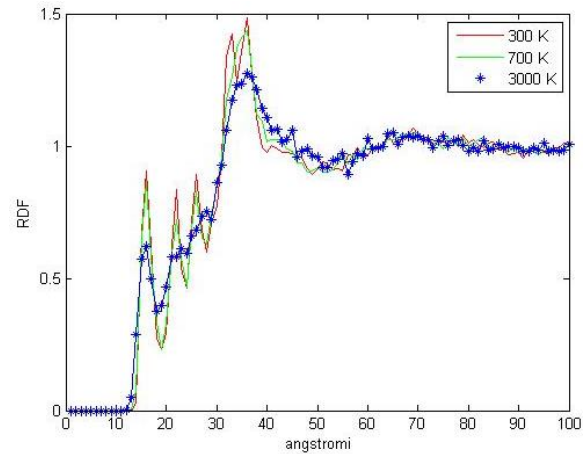


Fig. 17. The total radial distribution functions at 300, 700 and 3000K.

Table 2 presents the first three coordination radii, for the above-mentioned four temperatures. The third coordination radius is given only informatively.

Bond	3000 K			1000 K			700 K			300 K		
	R1	R2	R3	R1	R2	R3	R1	R2	R3	R1	R2	R3
Al-Al	3.74	6.30	8.46	3.78	6.52	-	3.79	6.18	8.53	3.72	6.00	8.14
Li-Li	2.70	5.44	8.30	-	-	-	2.54	6.32	8.21	2.50	5.05	6.99
Al-Li	3.09	6.48	8.69	-	-	-	3.12	6.09	8.21	3.23	6.07	8.12
O-Al	2.03	4.36	6.87	2.13	4.36	6.90	2.13	4.38	6.76	2.10	4.43	6.92
O-P	1.50	3.92	6.34	1.50	3.97	6.09	1.53	4.02	6.28	1.48	3.99	6.37
O-Li	2.01	4.11	6.71	2.01	4.27	6.48	1.94	4.29	6.53	1.92	4.38	6.64
O-O	2.52	4.91	7.43	2.50	4.96	7.43	2.52	5.03	7.29	2.54	5.01	7.43
P-Al	3.53	5.63	7.56	3.51	4.98	7.79	3.55	5.08	7.70	3.53	5.17	7.77
P-Li	3.03	6.76	9.71	3.12	5.93	7.61	3.12	6.20	-	3.12	5.77	7.20
P-P	3.19	4.41	7.17	3.26	4.43	7.13	3.21	4.45	7.29	3.23	4.36	7.17

The experimental data related to P-O, Li-O and Na-O bonds are presented as follows.

The phosphorous atom contains five valence electrons, and yet maintains a tetrahedral hybridization such that the P-O bonds are intrinsically anisotropic. In P_2O_5 crystal there are 2 phosphorous and 4 oxygen sites, in which the oxygen sites are classified into 2-bonded oxygen and 2 double bonded oxygen sites. Experimental data reveals that appears a wide distribution in P-O bond length; $r(P-BO) = 0.1637, 0.1588, 0.1571, 0.1527$ nm and $r(P=DBO) = 0.1492, 0.1426$ nm [10].

In the single component P glass the tetrahedral hybridization is clearly evident with three of the P-O bonds being bridging (with a P-O bond distance of 1.581 Å) along with a single terminal P-O bond (with a P-O distances of 1.432 Å) [11].

For lithium-phosphate systems, the average Li-O distance of 2.25 Å for the metaphosphate composition ($x=0.5$) is longer than the 2.03 Å reported in the neutron diffraction study of $LiPO_3$ glass, [12] or the average 1.96 Å Li-O bond distance observed for crystalline $LiPO_3$. Based on molecular orbital calculations, Uchino and Ogata reported that Li and Na ions interacted equally with the two kind (double bonded and/or non bonded) of terminal atoms of oxygen in a PO_4 unit but K and Rb ions interacted favorably with one of the two terminal atoms of oxygen [12]. That means that in the case of chosen system, which contains lithium, the bond lithium-oxygen-phosphorus is identical for both cases.

The results of our model places the radius of P-O bond between these experimental values for bonded and double bonded oxygen.

4. Conclusions

The two-body potential employed in the simulation of ternary $Li_2O-Al_2O_3-P_2O_5$ glass reproduces well the structural features such as pair and cumulative distribution functions. The simulated model is also in good agreement with the experimental X-ray and neutron diffraction data.

In the case of P-O bond the predicted value at 700K is near to the experimental one, for single bond. For 300K temperature it was calculated a value nearer to experimental double bonded one. In all temperature range the radius of Li-O bond is equally for both kinds of terminal oxygen atoms.

References

- [1] K. Hirao, N. Soga, J. of Non Cryst. Solids, **84**, 61 (1986).
- [2] G. G Boiko, M. Liska, B. Hatalova, XV-teen Int. Congress on Glass, Leningrad, 1a, 210 (1989).
- [3] Y. Benino, N. Soga, K. Hirao, XVI-teen Int. Congress on Glass, Madrid, 27, 1992.
- [4] N. Iwamoto, J. of Non Cryst. Solids **95-96**, 233 (1987).
- [5] T. P. Soules, J. of Non Cryst. Solids **49**, 29 (1982).
- [6] H. Matsumoto, Y. Shigesato, I. Yasui, Phys. Chem. Glasses **37**(5), 212 (1996).
- [7] M. D. Ingram, Phys. Chem. Glasses **28**(6), 215 (1987).
- [8] J. Habasaki, J. of Non Cryst. Solids **183**, 12 (1995).
- [9] M. N. Tomozawa, J. of Non Cryst. Solids **152**, 29 (1993).
- [10] S. W. Martin, A. Jha, N. M. Ravindra, Materials and systems **1**, 567 (2006).
- [11] T. M. Alam, J.-J. Liang, R. T. Cygan, Phys. Chem. Chem. Phys. **2**, 4427 (2000).
- [12] T. Uchino, Y. Ogata, J. Non-Cryst Solids **191**, 56 (1995).

*Corresponding author: savabogdanalexandru@yahoo.com